



Defence Research and  
Development Canada

Recherche et développement  
pour la défense Canada



# **Miniaturization of 3-dB/90° and 180° power splitters using microstrip technology**

Mathieu Caillet, Michel Clénet and Yahia M. M. Antar

**Defence R&D Canada – Ottawa**

TECHNICAL MEMORANDUM

DRDC Ottawa TM 2007-257

November 2007

Canada



# **Miniaturization of 3-dB / 90° and 180° power splitters using microstrip technology**

Mathieu Caillet  
Royal Military College of Canada

Michel Clénet  
Defence R&D Canada – Ottawa

Yahia M. M. Antar  
Royal Military College of Canada

**Defence R&D Canada – Ottawa**

Technical Memorandum

DRDC Ottawa TM 2007-257

November 2007

Co-author

*Original signed by Michel Clénet*

---

Michel Clénet

Approved by

*Original signed by Bill Katsube*

---

Bill Katsube  
SH CNEW

Approved for release by

*Original signed by Pierre Lavoie*

---

Pierre Lavoie  
Chairman DRP

- © Her Majesty the Queen in Right of Canada as represented by the Minister of National Defence, 2007
- © Sa Majesté la Reine (en droit du Canada), telle que représentée par le ministre de la Défense nationale, 2007

# Abstract

---

This document reports on the analysis and design of miniaturized 3-dB / 90° and 180° power splitters. Several miniaturization techniques are presented, and were applied to the design of microstrip splitters.

Concerning the 3-dB / 180° splitters, two miniaturized microstrip circuits have been designed using two different methods. The first one is a Moore 2nd iteration fractal ring hybrid, of size  $23 \times 28 \text{ mm}^2$  (23 % of the conventional ring hybrid area) with similar performance over the 1.15-1.6 GHz frequency band. Over this band, characterization has shown a maximum 3-dB coupling imbalance of 1 dB and an output phase difference varying by  $22^\circ (\pm 11^\circ)$ . The second proposed circuit is an H-shaped aperture-coupled transition, of compact size and wide frequency bandwidth. Its size is  $23 \times 30 \text{ mm}^2$ , including the slot and matching network. Measurements revealed a maximum 3-dB imbalance of 0.3 dB and an output phase difference fluctuation of  $1^\circ (\pm 0.5^\circ)$  over the 1.15-1.6 GHz band.

Regarding the 90° splitters, two miniaturization methods have been investigated to reduce the size of a branch-line hybrid. The first technique is based on fractal geometries as for the 180° splitter. A Sierpinski 2-nd iteration fractal branch-line hybrid has been simulated and showed a coupling imbalance of 0.4 dB and a phase difference variation of  $1^\circ (\pm 0.5^\circ)$  over a 10 % bandwidth. Its size is about 50 % of the area of the branch-line hybrid. The second miniaturization technique that has been investigated is founded on lumped distributed elements to reduce the size of a microstrip line. The possible size reduction is 50 % as well.

# Résumé

---

Le présent document porte sur l'analyse et la conception de diviseurs de puissance 3-dB / 90° et 180° miniatures. Plusieurs techniques de miniaturisation sont décrites, et elles ont été appliquées à la conception de diviseurs de puissance microruban.

Concernant les diviseurs de puissance 3 dB / 180°, deux circuits microrubans miniatures ont été conçus en utilisant deux méthodes différentes. Le premier circuit est un diviseur hybride en anneau à géométrie fractale de la 2ème itération de Moore, mesurant  $23 \times 28 \text{ mm}^2$  (23 % de la superficie d'un coupleur hybride en anneau classique), et offre des performances similaires sur la bande de fréquences 1,15-1,6 GHz. Sur cette bande, les mesures ont montré un déséquilibre du couplage à 3 dB de 1 dB maximum et une variation de la différence des phases de sortie de  $22^\circ (\pm 11^\circ)$ . Le deuxième circuit proposé est une transition ligne-fente-ligne à ouverture en H, compacte et ayant une bande de fréquence large. Il mesure  $23 \times 30 \text{ mm}^2$ , fente et réseau d'adaptation compris. Les mesures ont révélé un déséquilibre du couplage à 3 dB de 0,3 dB maximum et une variation de la différence des phases de sortie de  $1^\circ (\pm 0,5^\circ)$  sur la bande 1,15-1,6 GHz.

Quand aux diviseurs de puissance 3 dB / 90°, deux méthodes de miniaturisation ont été étudiées en vue de réduire la taille d'un coupleur hybride à quadrature. La première technique est basée sur une géométrie fractale comme dans le cas du diviseur 180°. Un coupleur hybride à quadrature a été conçu avec une géométrie fractale de la 2ème itération de Sierpinski, et un déséquilibre du couplage à 3 dB de 0,4 dB maximum avec une variation de la différence des phases de sortie de 1° ( $\pm 0,5^\circ$ ) a été obtenu en prenant en compte une largeur de bande de 10 %. Sa superficie est environ 50 % celle du diviseur hybride à quadrature classique. La deuxième technique de miniaturisation qui a été étudiée est basée sur l'utilisation d'éléments distribués semi-localisés pour réduire la taille d'une ligne microruban. La réduction de taille réalisable est également de 50 %.

# Executive summary

---

## Miniaturization of 3-dB / 90° and 180° power splitters using microstrip technology

Mathieu Caillet, Michel Clénet, Yahia M. M. Antar; DRDC Ottawa TM 2007-257; Defence R&D Canada – Ottawa; November 2007.

**Background:** 90° and 180° power splitters are commonly used in the design of circularly polarized antenna feeding circuits. Baluns and hybrids are easily realized using planar circuit technology as they employ only transmission lines without additional components. However, as the electrical lengths of the transmission line elements are either 90° or 270°, such circuits consume a significant amount of circuit area, especially at lower frequencies. This report shows the development of miniaturized 3-dB / 90° and 180° power splitters. Electromagnetic simulation and experimental results were used to confirm the design approach for hybrids operating at 1.37 GHz. The frequency response of the proposed hybrids is similar to conventional hybrids.

**Principal results:** Concerning the 3-dB / 180° splitters, two miniaturized microstrip circuits have been designed using two different methods. The first one is a Moore 2nd iteration fractal ring hybrid, of size  $23 \times 28 \text{ mm}^2$  (23 % of the conventional ring hybrid area) with similar performance over the 1.15-1.6 GHz frequency band. Over this band, characterization has shown a maximum 3-dB coupling imbalance of 1 dB and an output phase difference varying by 22° ( $\pm 11^\circ$ ). The second proposed circuit is an H-shaped aperture-coupled transition, of compact size and wide frequency bandwidth. Its size is  $23 \times 30 \text{ mm}^2$ , including the slot and matching network. Measurements revealed a maximum 3-dB imbalance of 0.3 dB and an output phase difference fluctuation of 1° ( $\pm 0.5^\circ$ ) over the 1.15-1.6 GHz band.

Regarding the 90° splitters, two miniaturization methods have been investigated to reduce the size of a branch-line hybrid. The first technique is based on fractal geometries as for the 180° splitter. A Sierpinski 2-nd iteration fractal branch-line hybrid has been simulated and showed a coupling imbalance of 0.4 dB and a phase difference variation of 1° ( $\pm 0.5^\circ$ ) over a 10 % bandwidth. Its size is about 50 % of the area of the branch-line hybrid. The second miniaturization technique that has been investigated is founded on lumped distributed elements to reduce the size of a microstrip line. The possible size reduction is 50 % as well.

**Significance of results:** The methods used here consist of reducing the surface area occupied by conventional structures through the use of space-filling curves and distributed lumped elements having the same electrical characteristics. Additionally, a microstrip aperture-coupled transition has been designed, providing a compact solution for a 3-dB / 180°

power splitter. The achieved size is 23 to 50 % the area of conventional geometries, with a frequency response similar to conventional circuits. Numerous other methods have been developed to reduce the size of the balun and hybrid topologies: use of metamaterials, planar artificial transmission lines, Coplanar Printed Waveguide (CPW), etc. Usually, the size reduction is around 50 %.

**Future work:** It is planned to do some tests with a substrate with dielectric losses lower than the FR4 substrate to see if the insertion loss could be improved. Moreover, other techniques can further reduce more the size of the circuits. For instance, coupled lines are integrable using Low Temperature Co-fired Ceramic (LTCC). Finally, the presented results concern narrowband circuits; for broad frequency band applications, the obtained performances are not sufficient, and the studied methods could be investigated as well to design wide-band circuits.



# Sommaire

---

## Miniaturization of 3-dB / 90° and 180° power splitters using microstrip technology

Mathieu Caillet, Michel Clénet, Yahia M. M. Antar ; DRDC Ottawa TM 2007-257 ; R & D pour la défense Canada – Ottawa ; novembre 2007.

**Contexte :** Les diviseurs de puissance 90° et 180° sont couramment utilisés dans la conception de circuits d'alimentation d'antenne à polarisation circulaire. Des diviseurs symétriques Balun et des coupleurs hybrides peuvent être facilement produits à l'aide de la technologie des circuits planaires car ils n'utilisent que des lignes de transmission sans éléments additionnels. Cependant, comme les longueurs électriques des éléments de ligne de transmission sont de 90° ou 270°, ces circuits occupent une superficie importante, particulièrement aux fréquences basses. Le présent rapport traite du développement de diviseurs de puissance 3 dB / 90° et 180° miniatures. La simulation électromagnétique et les résultats d'expériences ont été utilisés pour valider la méthode de conception des coupleurs hybrides fonctionnant à 1,37 GHz. La réponse en fréquence des coupleurs hybrides proposés est similaire à celle des coupleurs hybrides classiques.

**Résultats principaux :** Concernant les diviseurs de puissance 3 dB / 180°, deux circuits microrubans miniatures ont été conçus en utilisant deux méthodes différentes. Le premier circuit est un diviseur hybride en anneau à géométrie fractale de la 2ème itération de Moore, mesurant  $23 \times 28 \text{ mm}^2$  (23 % de la superficie d'un coupleur hybride en anneau classique), et offre des performances similaires sur la bande de fréquences 1,15-1,6 GHz. Sur cette bande, les mesures ont montré un déséquilibre du couplage à 3 dB de 1 dB maximum et une variation de la différence des phases de sortie de 22° ( $\pm 11^\circ$ ). Le deuxième circuit proposé est une transition ligne-fente-ligne à ouverture en H, compacte et ayant une bande de fréquence large. Il mesure  $23 \times 30 \text{ mm}^2$ , fente et réseau d'adaptation compris. Les mesures ont révélé un déséquilibre du couplage à 3 dB de 0,3 dB maximum et une variation de la différence des phases de sortie de 1° ( $\pm 0,5^\circ$ ) sur la bande 1,15-1,6 GHz. Quand aux diviseurs de puissance 3 dB / 90°, deux méthodes de miniaturisation ont été étudiées en vue de réduire la taille d'un coupleur hybride à quadrature. La première technique est basée sur une géométrie fractale comme dans le cas du diviseur 180°. Un coupleur hybride à quadrature a été conçu avec une géométrie fractale de la 2ème itération de Sierpinski, et un déséquilibre du couplage à 3 dB de 0,4 dB maximum avec une variation de la différence des phases de sortie de 1° ( $\pm 0,5^\circ$ ) a été obtenu en prenant en compte une largeur de bande de 10 %. Sa superficie est environ 50 % celle du diviseur hybride à quadrature classique. La deuxième technique de miniaturisation qui a été étudiée est basée sur l'utilisation d'éléments distribués semi-localisés pour réduire la taille d'une ligne microruban. La réduction de taille réalisable est également de 50 %.

**Portée des résultats :** Les méthodes présentées ici consistent à réduire la surface occupée par les structures classiques en ayant recours à des géométries fractales et à des éléments distribués semi-localisés ayant les mêmes caractéristiques électriques. De plus, une transition ligne-fente-ligne à couplage à travers une ouverture offre une solution compacte pour un diviseur de puissance 3 dB / 180°. Les tailles obtenues sont de 23 à 50 % celle des structures classiques, avec une réponse en fréquence similaire. De nombreuses autres méthodes ont été présentées dans la littérature en vue de réduire la taille des topologies des diviseurs symétriques Balun et des coupleurs hybrides : utilisation de métamatériaux, lignes de transmission artificielles planaires, circuits imprimés coplanaires (CPW), etc. Habituellement, la réduction de la taille est d'environ 50 %.

**Perspectives :** Il pourrait être intéressant de faire des essais avec un substrat dont les pertes diélectriques sont plus faibles que celles du substrat FR4 utilisé, afin de déterminer si les pertes d'insertion pourraient être réduites. En outre, il est possible d'utiliser d'autres technologies pour réduire davantage la taille des circuits. Par exemple, les lignes couplées peuvent être intégrées à l'aide de céramique pressée à basse température (LTCC). Enfin, les résultats présentés ont trait à des circuits à bande étroite. Pour les applications à large bande de fréquences, les performances obtenues ne sont pas suffisantes, et l'utilisation des méthodes étudiées pourrait être envisagée également pour la conception de circuits large-bande.

# Table of contents

---

Abstract . . . . .	i
Résumé . . . . .	i
Executive summary . . . . .	iii
Sommaire . . . . .	v
Table of contents . . . . .	vii
List of figures . . . . .	ix
1 Introduction . . . . .	1
2 Simulation and characterization of 3-dB / 180° power splitters . . . . .	2
2.1 The microstrip ring hybrid . . . . .	2
2.1.1 Simulations . . . . .	3
2.1.2 Characterization and results . . . . .	3
2.2 Fractal microstrip 180° hybrid . . . . .	7
2.2.1 Moore 1-st iteration fractal hybrid . . . . .	7
2.2.2 Moore 2-nd iteration fractal hybrid . . . . .	9
2.3 Double layer aperture-coupled transition structure . . . . .	11
2.3.1 Simulations . . . . .	15
2.3.2 Characterization and results . . . . .	17
2.4 Concluding remarks . . . . .	17
3 Simulation and characterization of 3-dB / 90° power splitters . . . . .	22
3.1 Conventional 3-dB / 90° branch-line hybrid . . . . .	22
3.2 Fractal printed hybrid . . . . .	24
3.2.1 Sierpinski 1-st iteration fractal hybrid . . . . .	24
3.2.2 Sierpinski 2-nd iteration fractal hybrid . . . . .	26

3.3	Lumped distributed elements . . . . .	27
3.4	Concluding remarks . . . . .	28
4	Conclusions and future work . . . . .	29
	References . . . . .	30

# List of figures

---

Figure 1:	Microstrip ring hybrid on 60-mil FR4 substrate . . . . .	2
Figure 2:	Simulated ring hybrid S-parameter magnitudes . . . . .	3
Figure 3:	Simulated ring hybrid outputs: (a) magnitude and (b) phase . . . . .	4
Figure 4:	Fabricated microstrip ring hybrid on 60-mil FR4 substrate . . . . .	5
Figure 5:	Characterization results of the ring hybrid S-parameters: (a) magnitude and (b) phase outputs . . . . .	6
Figure 6:	Moore 1-st iteration fractal 180° hybrid on 60-mil FR4 substrate . . . . .	7
Figure 7:	Moore 1-st iteration fractal 180° hybrid S-parameters: (a) magnitude and (b) phase outputs . . . . .	8
Figure 8:	Fabricated Moore 1-st iteration fractal hybrid on 60-mil FR4 substrate . . . . .	9
Figure 9:	Characterization results of the Moore 1-st iteration fractal hybrid S-parameters: (a) magnitude and (b) phase outputs . . . . .	10
Figure 10:	Moore 2-nd iteration fractal 180° hybrid on 30-mil FR4 substrate . . . . .	11
Figure 11:	Moore 2-nd iteration fractal 180° hybrid S-parameters: (a) magnitude and (b) phase outputs . . . . .	12
Figure 12:	Fabricated Moore 2-nd iteration fractal hybrid on 30-mil FR4 substrate . . . . .	13
Figure 13:	Characterization results of the Moore 2-nd iteration fractal hybrid S-parameters: (a) magnitude and (b) phase outputs . . . . .	14
Figure 14:	Aperture-coupled transition on 60-mil FR4 double layer substrate . . . . .	15
Figure 15:	Linear aperture-coupled transition S-parameters: (a) magnitude and (b) phase outputs. $ S_{21} $ and $ S_{31} $ curves are overlaid. . . . .	16
Figure 16:	H-shaped aperture-coupled transition on 60-mil FR4 double layer substrate – Top view . . . . .	17
Figure 17:	H-shaped aperture-coupled transition S-parameters: (a) magnitude and (b) outputs phase. $ S_{21} $ and $ S_{31} $ curves are overlaid. . . . .	18
Figure 18:	H-shaped aperture-coupled transition structure . . . . .	19

Figure 19: H-shaped aperture-coupled transition prototype (a) top and (b) bottom view – Thin lines show the position of the slot in the ground plane . . . .	19
Figure 20: Characterization results of the H-shaped aperture-coupled transition S-parameters: (a) magnitude and (b) phase outputs . . . . .	20
Figure 21: Hybrid designs on same scale using FR4 substrate . . . . .	21
Figure 22: Microstrip branch-line hybrid on 60-mil FR4 substrate . . . . .	22
Figure 23: Branch-line hybrid simulated S-parameters: (a) magnitude and (b) phase outputs . . . . .	23
Figure 24: Sierpinski 1-st iteration 90° fractal hybrid on 60-mils FR4 substrate . . .	24
Figure 25: Sierpinski 1-st iteration 90° fractal hybrid simulated S-parameters: (a) magnitude and (b) phase outputs . . . . .	25
Figure 26: Sierpinski 2-nd iteration 90° fractal hybrid on 30-mil FR4 substrate . . .	26
Figure 27: Hybrid designs on same scale using FR4 substrate . . . . .	27
Figure 28: Size reduction scheme using lumped distributed elements. (a) Conventional transmission line. (b) Equivalent transmission line with a series transmission line and two open stubs. . . . .	27

# 1 Introduction

---

$90^\circ$  and  $180^\circ$  power splitters are commonly used in the design of circularly polarized antenna feeding circuits. For instance, a quadrifilar helix antenna [1] needs to be fed by a network having one input port and four output ports with equal magnitude and  $90^\circ$  phase difference between each port. Baluns and hybrids are frequently used due to simple designs and ease of realization using a standard printed circuit board fabrication process. However, the main limitation for their use lies in the large surface area required, especially at lower frequencies.

Numerous methods have been developed to reduce the size of these topologies [2, 3, 4]. Recently, a novel method based on the use of space-filling curves has been proposed by Ghali and Moselhy [5]. This method consists of choosing a fractal geometry and the associated iteration number to determine the corresponding area reduction. It allows one to reduce greatly the occupied area of baluns and hybrids [6]. Additionally, the use of distributed lumped elements is an interesting technique to reduce the length of a transmission line [7]. Particularly, it can be applied to the miniaturization of branch-line hybrids.

This report describes the analysis and design of miniaturized 3-dB power splitters. The 3-dB /  $180^\circ$  power splitters are presented in Section 2 and the 3-dB /  $90^\circ$  power splitters in Section 3. Simulations and characterization results are provided for several designs. Conclusions and future plan are given in Section 4.

## 2 Simulation and characterization of 3-dB / 180° power splitters

---

Two different types of compact circuits are reviewed here that evenly split the power and provide a 180° phase difference between the two outputs. The first circuit is the conventional ring hybrid, which has been miniaturized using fractal geometry. The second splitter is an aperture-coupled transition built on a double layer substrate technology, which is of compact size. The performances are evaluated between 1.15 and 1.6 GHz, and the center frequency is 1.37 GHz. All simulations have been performed by taking material losses into account.

### 2.1 The microstrip ring hybrid

The 180° hybrid junction includes a ring, with an impedance of 70.7 Ω and a perimeter of 1.5 λ<sub>g</sub> (λ<sub>g</sub> is the guided wavelength at 1.37 GHz), and 4 input lines of 50 Ω. This forms a four-port network with a 180° phase shift between two specified output ports. The distance between the ports in the top ring is λ<sub>g</sub>/4.

Figure 1 shows the geometry and the convention for the ports. If the input is applied to port 1, the power will be evenly split into two components with a 180° phase difference at ports 3 and 4, and port 2 will be isolated. Details on the functioning of the 180° hybrid can be found in [8].

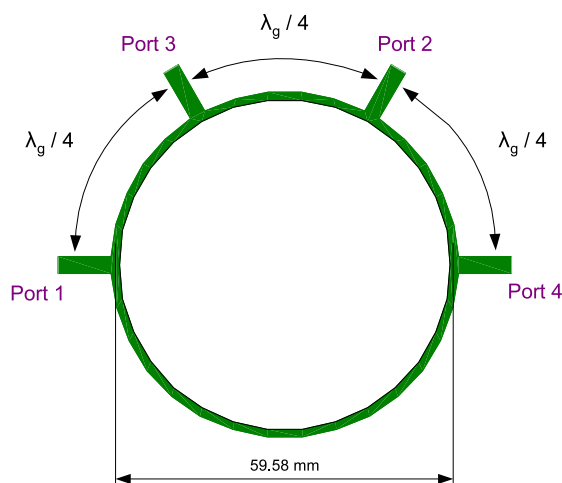


**Figure 1:** Microstrip ring hybrid on 60-mil FR4 substrate



## 2.1.1 Simulations

Simulation results of S-parameters obtained on a 60-mil FR4 substrate ( $\epsilon_r = 4.4$  and  $tg \delta = 0.009$ ) with the dimensions of Fig. 1 are presented in Fig. 2. Two commercial simulation tools have been used to compare results; Ansoft Designer, based on the method of moments, and Ansoft HFSS, based on the finite element method. The model developed with Designer has infinite substrate and ground plane, while with HFSS the size of the substrate and ground plane is  $101.6 \times 101.6 \text{ mm}^2$ . The  $50 \Omega$  and  $70.7 \Omega$  lines are  $2.9 \text{ mm}$  and  $1.4 \text{ mm}$  wide respectively. Simulation results agree quite well for both simulation methods. One can notice a difference on return loss.

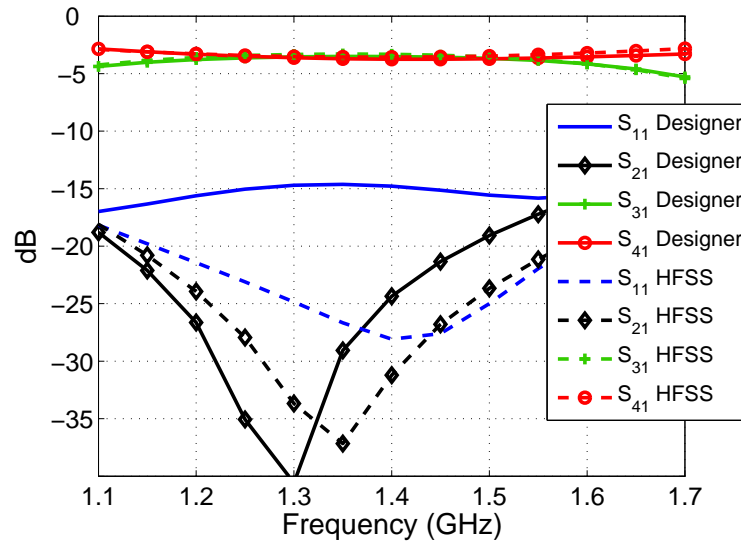
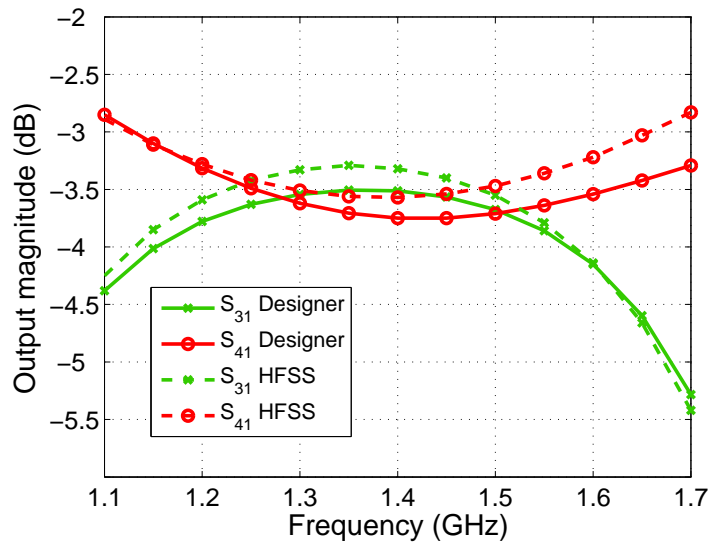


**Figure 2:** Simulated ring hybrid S-parameter magnitudes

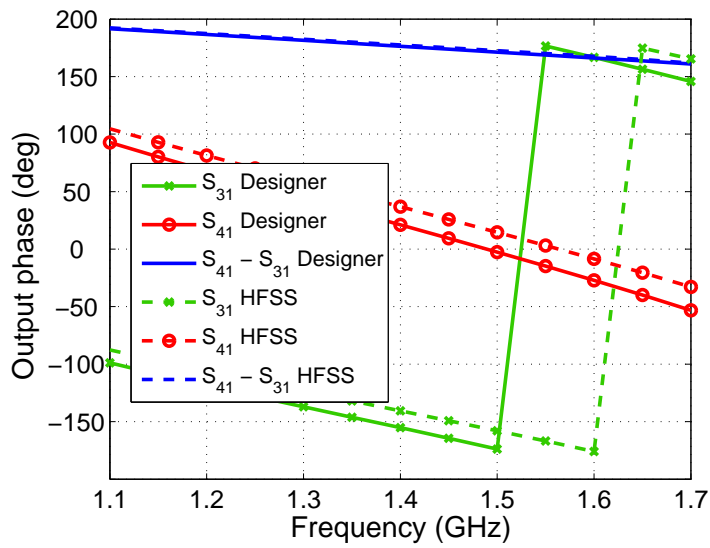
Magnitude and phase data are given in Fig. 3. Between 1.15 and 1.6 GHz, a 3-dB coupling with maximum amplitude unbalance of less than 0.9 dB is obtained and the phase variation is  $23^\circ (\pm 11.5^\circ)$  over the frequency band.

## 2.1.2 Characterization and results

A prototype of the ring hybrid has been fabricated using a 60-mil FR4 substrate (Fig. 4). The characterization results for magnitude and phase are shown in Fig. 5. The return loss is  $-25.9 \text{ dB}$  at  $1.4 \text{ GHz}$ , which is in agreement with simulation ( $-28.1 \text{ dB}$ ). Comparison of simulation (Ansoft Designer) and measured results for output S-parameters are given in Table 1. The data are close to perfect agreement.



(a)



(b)

**Figure 3:** Simulated ring hybrid outputs: (a) magnitude and (b) phase

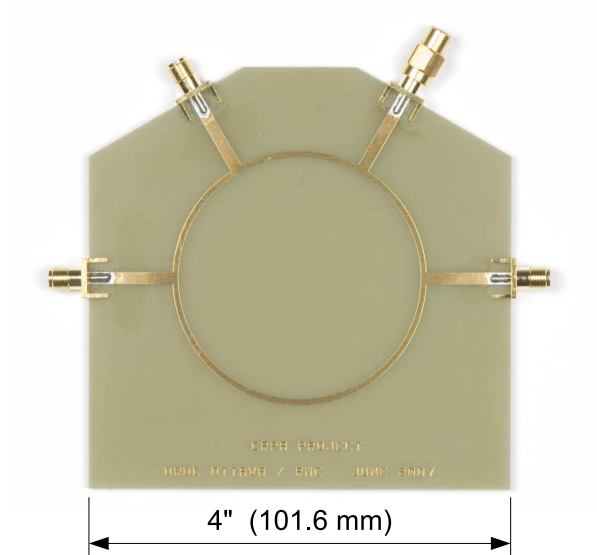
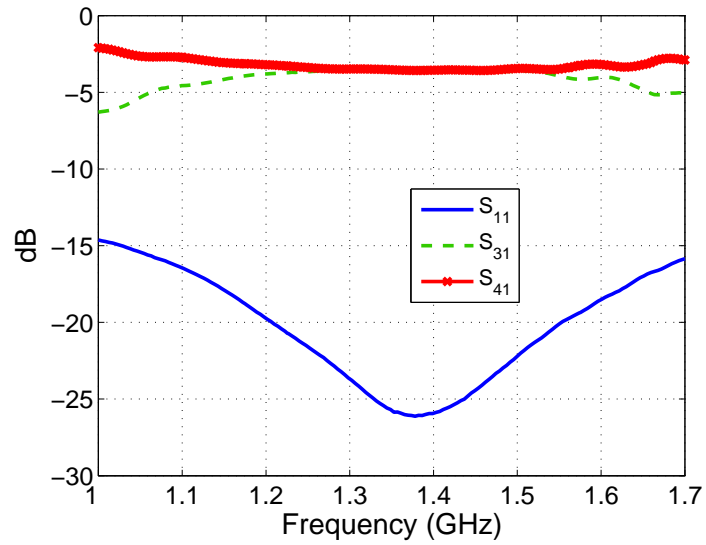


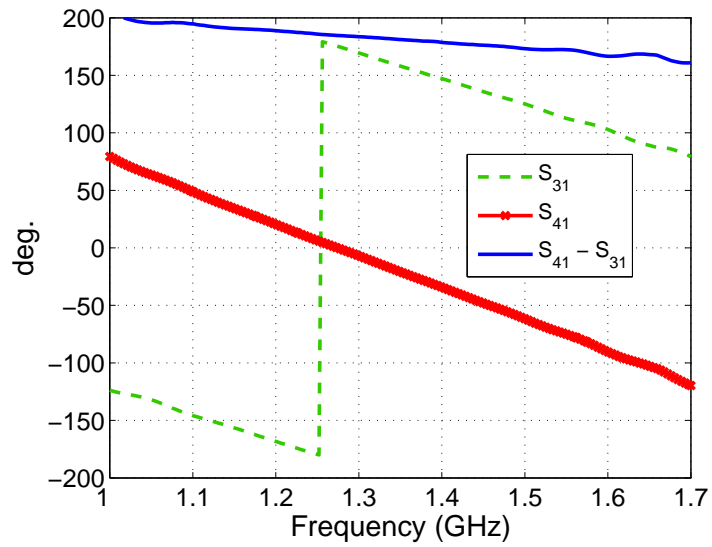
**Figure 4:** Fabricated microstrip ring hybrid on 60-mil FR4 substrate

	Amplitude $S_{31}/S_{41}$ (dB)		Phase diff. ( $^{\circ}$ )	
	Simu.	Charact.	Simu.	Charact.
1.15 GHz	-4.02/-3.10	-4.14/-3.07	189.1	190.7
1.35 GHz	-3.51/-3.71	-3.44/-3.53	179.0	181.2
1.6 GHz	-4.15/-3.54	-4.03/-3.18	166.2	166.6

**Table 1:** Comparison of simulated and characterized results for the ring hybrid



(a)



(b)

**Figure 5:** Characterization results of the ring hybrid S-parameters: (a) magnitude and (b) phase outputs

## 2.2 Fractal microstrip 180° hybrid

In [6], some fractal geometries are presented to design compact hybrids. These are called Moore, Sierpinski, and Minkowski constructions. Among these shapes, Moore's allows the best reduction in area and thus has been selected to reduce the size of the 180° ring hybrid. The implementation and design are described in this section.

### 2.2.1 Moore 1-st iteration fractal hybrid

The first iteration of Moore's geometry has the shape of the letter 'I' (Fig. 6). One can note that this structure includes 16 segments. To find the length of a segment, the equation  $8 \text{ segments} = 3 \lambda_g / 4$  has to be solved. To take into account the width of the line, the length of the segment has to be shortened depending on the width of the line.

A ring hybrid has been implemented on a 60-mil FR4 substrate (Fig. 6). The impedance of the central line is  $70.7 \Omega$ , which corresponds to  $1.54 \text{ mm}$  for the selected substrate. The length of each segment has been adjusted to  $11.54 \text{ mm}$ . The four outputs have a  $50 \Omega$  impedance.

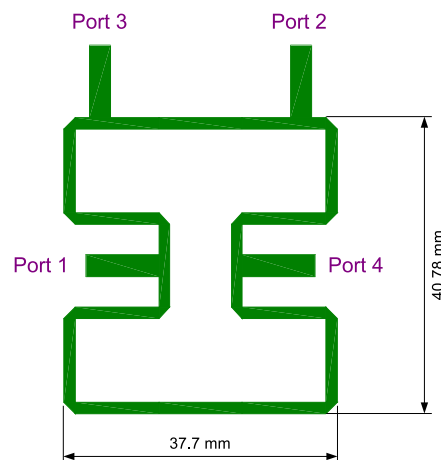
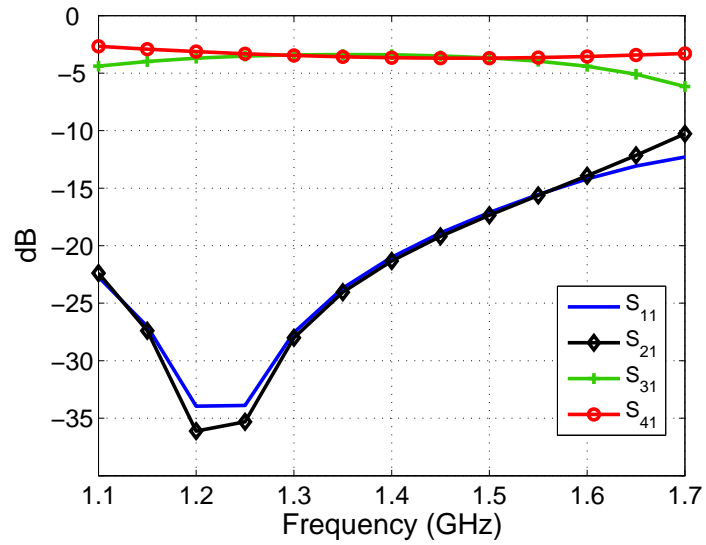


**Figure 6:** Moore 1-st iteration fractal 180° hybrid on 60-mil FR4 substrate

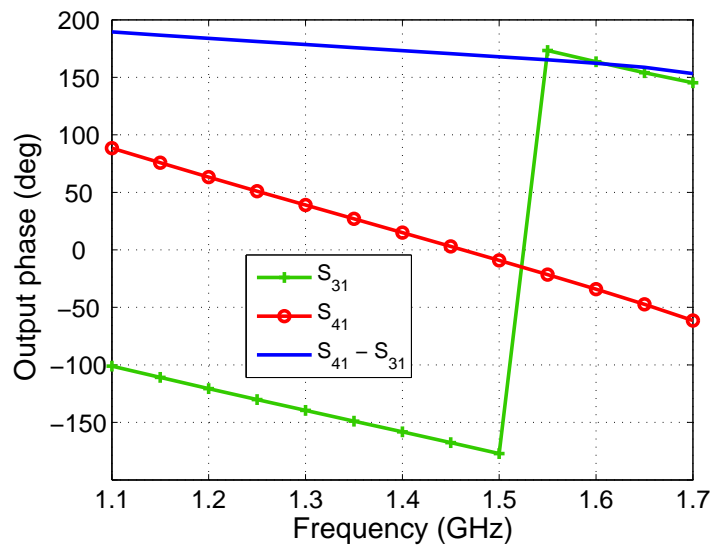
The simulated S-parameters for the designed circuit on a 60-mil FR4 substrate with the dimensions of Fig. 6 are presented in Fig. 7(a). Phase data are given in Fig. 7(b). Between 1.15 and 1.6 GHz, a 3-dB coupling with maximum amplitude unbalance of less than 1 dB is obtained and the phase variation is  $24^\circ (\pm 12^\circ)$  over the frequency band.

If the area of the ring hybrid is  $\pi.r^2$ , with  $r$  the radius of the ring, and the area of the Moore 1st iteration fractal hybrid is defined as  $a.b$ , with  $a$  and  $b$  the lengths of sides, the fractal geometry area is 55 % of the ring area.

A prototype has been built on a FR4 60-mil substrate (Fig. 8). The characterization results for magnitude and phase are shown in Fig. 9. The return loss is in agreement with



(a)



(b)

**Figure 7:** Moore 1-st iteration fractal  $180^\circ$  hybrid S-parameters: (a) magnitude and (b) phase outputs

simulation. Comparison of simulation and measured results are given in Table 2 for output magnitude and phase difference. A shift of  $-0.5$  dB can be noted for  $S_{31}$  compared to simulation, but not for  $S_{41}$ . As a consequence, the magnitude difference of 1 dB between  $S_{31}$  and  $S_{41}$  in simulation at 1.15 and 1.6 GHz increase to 1.5 dB in measurement. A shift of  $5^\circ$  is observed in the phase difference.



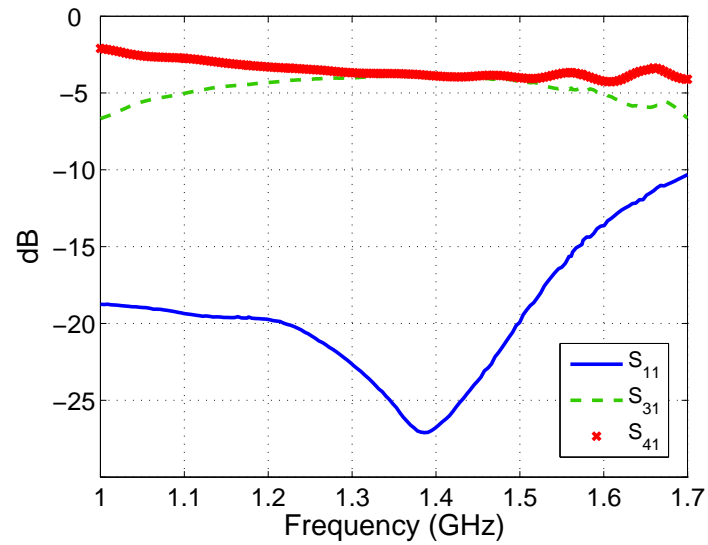
**Figure 8:** Fabricated Moore 1-st iteration fractal hybrid on 60-mil FR4 substrate

	Amplitude $S_{31}/S_{41}$ (dB)		Phase diff. ( $^\circ$ )	
	Simu.	Charact.	Simu.	Charact.
1.15 GHz	-3.98/-2.91	-4.56/-3.07	186.7	190.2
1.35 GHz	-3.38/-3.58	-3.90/-3.74	175.8	180.6
1.6 GHz	-4.41/-3.56	-5.00/-4.24	162.3	168.2

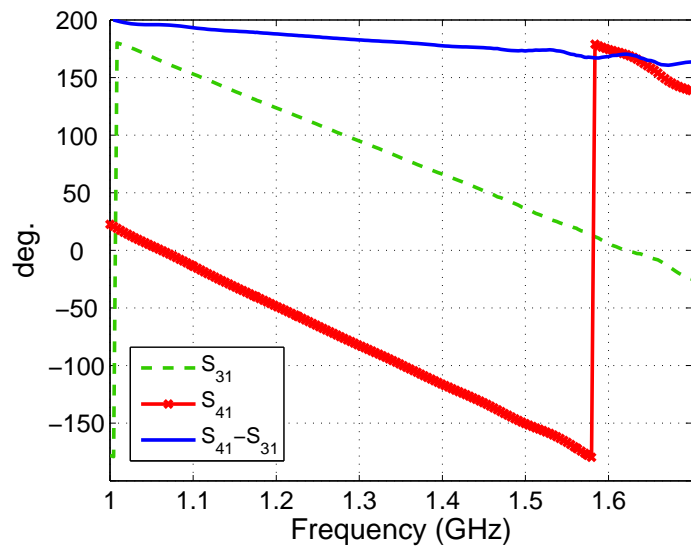
**Table 2:** Comparison of simulated and characterized results for the Moore 1-st iteration fractal hybrid

### 2.2.2 Moore 2-nd iteration fractal hybrid

The second iteration of the Moore's construction allows a higher reduction in the ring hybrid's area. Indeed, the perimeter of the central line is confined in a smaller surface because the construction includes more meanders (Fig. 10). This structure includes 64 segments, and 4 segments could be added in the center area to provide more room to the input and output lines and limit coupling between lines. In this case, the line length is around 2.4 mm at 1.37 GHz.



(a)



(b)

**Figure 9:** Characterization results of the Moore 1-st iteration fractal hybrid S-parameters: (a) magnitude and (b) phase outputs



So far in this report, ring hybrids have been implemented on 60-mil FR4 substrate. On this material, the trace width corresponding to the  $70.7 \Omega$  impedance equals  $1.54 \text{ mm}$ . However, due to small segment length, the use of such a width is not practicable. To avoid such problems, the coupler could be designed with a higher characteristic impedance ( $100 \Omega$  for instance) and with quarter-wave lines for matching. But at  $1.37 \text{ GHz}$ , the length of a quarter wave line is important (around  $30 \text{ mm}$ ). Another solution is to implement the coupler on a 30-mil FR4 substrate. In this case, the width of lines can be maintained for  $70.7 \Omega$  and no additional matching is needed. A segment of the fractal geometry on a 30-mil dielectric material is  $2.6 \text{ mm}$  long and  $0.77 \text{ mm}$  wide.

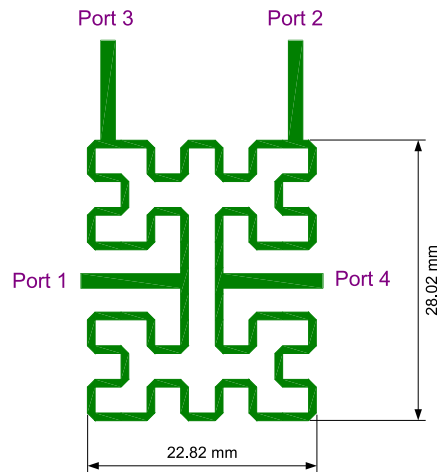


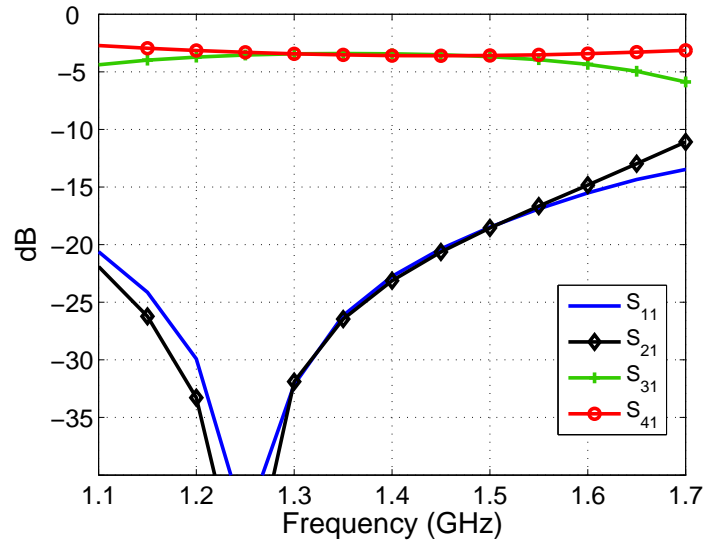
**Figure 10:** Moore 2-nd iteration fractal  $180^\circ$  hybrid on 30-mil FR4 substrate

Simulation results of S-parameters obtained for a 30-mil FR4 substrate with the dimensions of Fig. 10 are presented in Fig. 11(a). Phase data are given in Fig. 11(b). Between  $1.15$  and  $1.6 \text{ GHz}$ , a 3-dB coupling with maximum amplitude unbalance of less than  $1 \text{ dB}$  is obtained and the phase variation is  $24^\circ (\pm 12^\circ)$  over the frequency band. The performance is similar to that of the Moore 1-st iteration fractal hybrid realized on a 60-mil FR4 substrate. However, in the case of the Moore 2-nd iteration, the fractal geometry area is 23 % of the ring area.

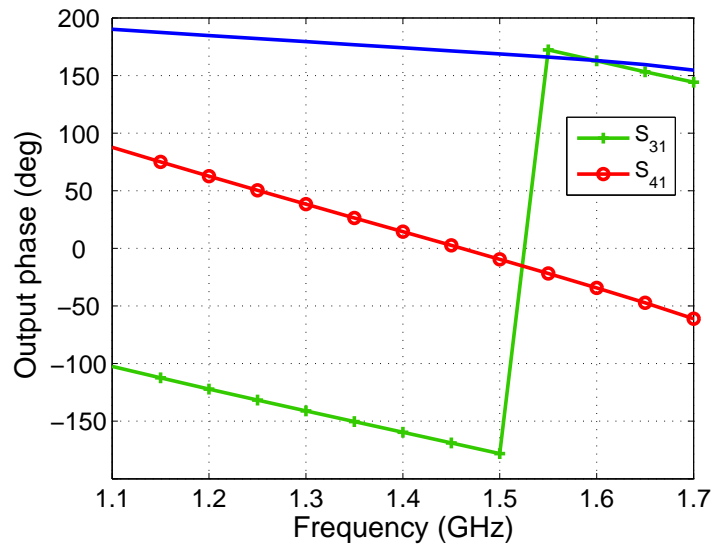
A prototype has been fabricated on an FR4 30-mil substrate (Fig. 12). The characterization results for magnitude and phase are shown in Fig. 13. The return loss is in agreement with simulation. Comparison of simulation and measured results are given in Table 3. The amplitude difference of  $1 \text{ dB}$  between  $S_{31}$  and  $S_{41}$  in simulation at  $1.15 \text{ GHz}$  is also observed in measurement. Here again, a shift of  $6^\circ$  is noted in the phase difference.

## 2.3 Double layer aperture-coupled transition structure

The aperture-coupled transition is another structure that can be used to build a  $180^\circ$  power splitter [9]. This structure includes two layers of substrate and a slot etched in the ground



(a)



(b)

**Figure 11:** Moore 2-nd iteration fractal  $180^\circ$  hybrid S-parameters: (a) magnitude and (b) phase outputs

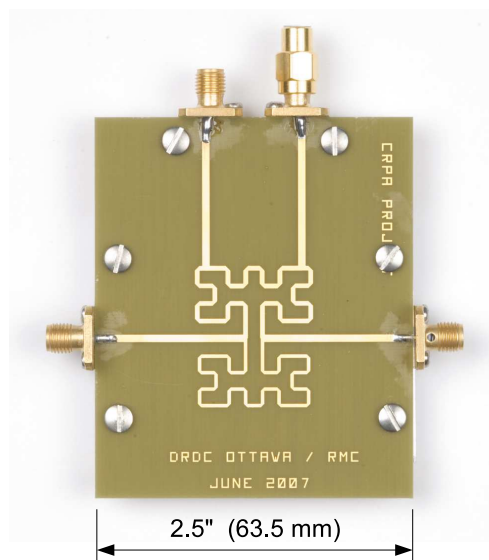
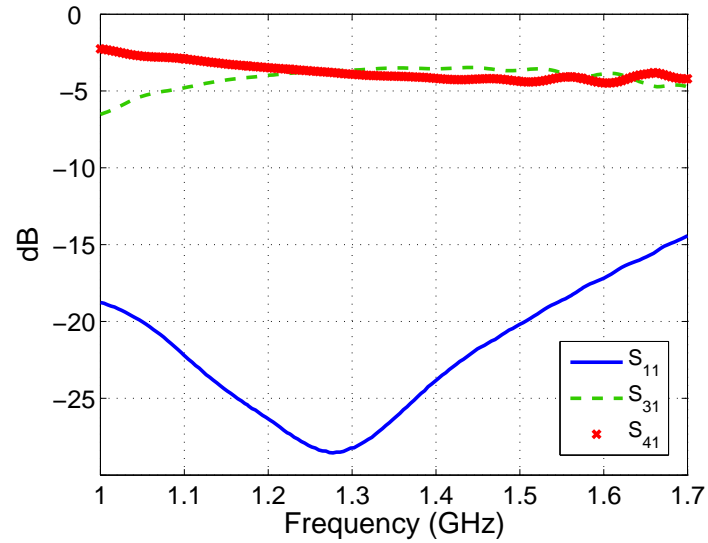


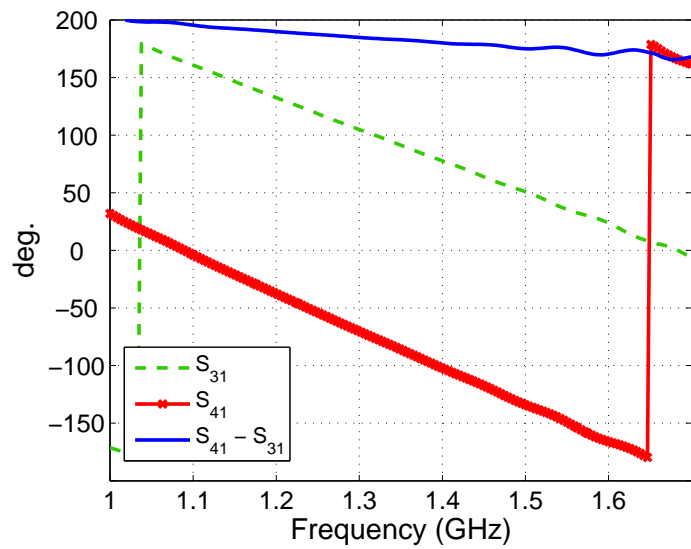
**Figure 12:** Fabricated Moore 2-nd iteration fractal hybrid on 30-mil FR4 substrate

	Amplitude $S_{31}/S_{41}$ (dB)		Phase diff. ( $^{\circ}$ )	
	Simu.	Charact.	Simu.	Charact.
1.15 GHz	-3.99/-2.95	-4.27/-3.25	187.4	192.3
1.35 GHz	-3.41/-3.53	-3.51/-4.03	176.7	182.8
1.6 GHz	-4.35/-3.43	-3.88/-4.48	163.0	170.4

**Table 3:** Comparison of simulated and characterized results for the Moore 2-nd iteration fractal hybrid



(a)



(b)

**Figure 13:** Characterization results of the Moore 2-nd iteration fractal hybrid  $S$ -parameters: (a) magnitude and (b) phase outputs

plane (Fig. 14). The feeding line (port 1) is located on the lower layer and the outputs (ports 2 and 3) are on the upper layer. A serial stub is needed on the lower layer to transform port 1 to  $50 \Omega$ . A quarter-wavelength line is placed on top of the slot between the two outputs to match the T-junction.

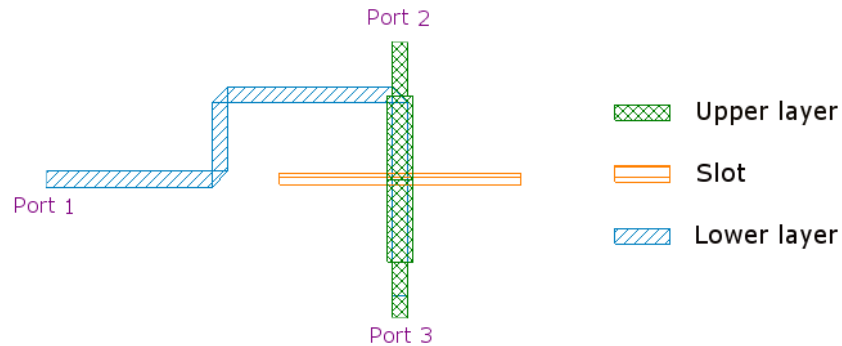


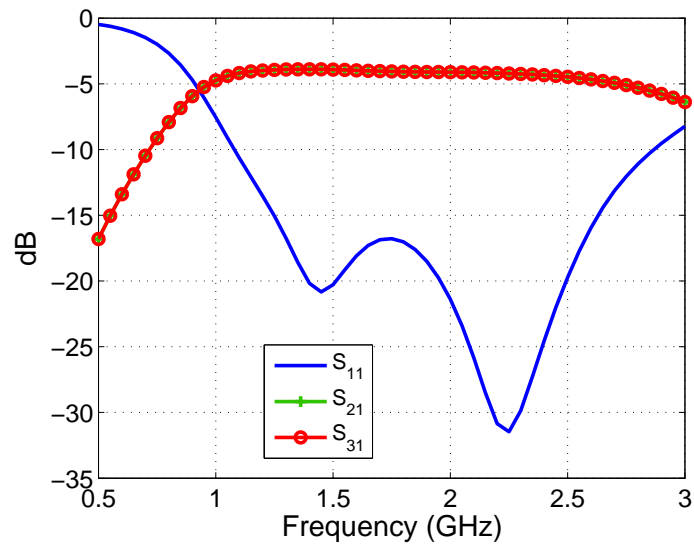
**Figure 14:** Aperture-coupled transition on 60-mil FR4 double layer substrate

### 2.3.1 Simulations

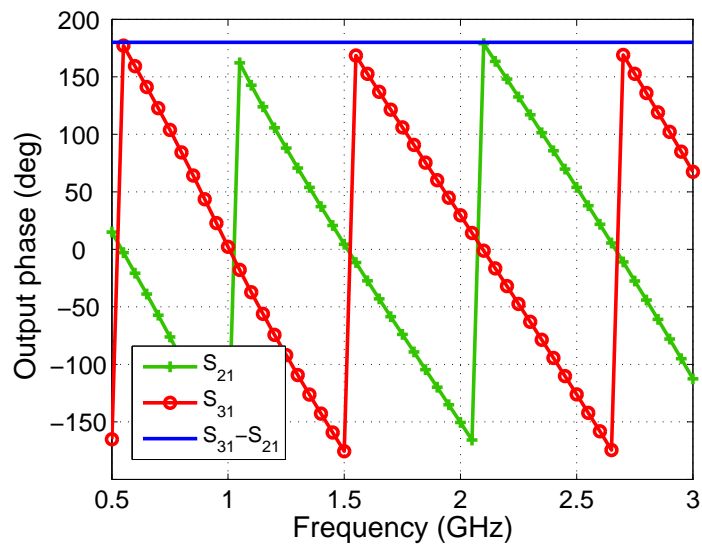
For an implementation with a 60-mil FR4 substrate, a  $2 - mm$  wide linear slot has been chosen. The length of the slot is  $44 mm$ , and the stub realized with a  $50 \Omega$  line is  $21 mm$  long. The quarter-wavelength line is  $4.8 mm$  wide and  $30 mm$  long.

Simulation results of S-parameters obtained with this geometry (Fig. 14) are presented in Fig. 15(a). Phase data are given in Fig. 15(b). Between 1.15 and 1.6 GHz, a 3-dB coupling with an amplitude unbalance of nearly  $0 dB$  is obtained and the phase variation is close to zero over the frequency band. This compact structure has good performance over a wide frequency band. Because the frequency band of the aperture-coupled transition is wider than the desired band (1.15-1.6 GHz), the slot, the quarter-wavelength line and the stub have been designed to shift the desired band to the lower band of the overall transition frequency band. This way the size of the slot is smaller than if this latter was designed to work at a center frequency of 1.37 GHz.

The size of the aperture-coupled transition can be further reduced by modifying the shape of the slot. Indeed, an H-shaped slot provides an improvement of the coupling [10], as well as reducing its length. The linear slot is  $44 mm$  long, the middle part of the H-shaped slot and the two arms are  $19 mm$  long (Fig. 16). The dimensions of the stub and the upper quarter-wavelength line remain identical. The H-shaped aperture-coupled transition simulation results (Fig. 17) are very similar to the linear aperture ones, except that the magnitude of outputs is around  $-3.7 dB$  instead of  $-4.0 dB$  in the case of the linear slot.



(a)



(b)

**Figure 15:** Linear aperture-coupled transition  $S$ -parameters: (a) magnitude and (b) phase outputs.  $|S_{21}|$  and  $|S_{31}|$  curves are overlaid.

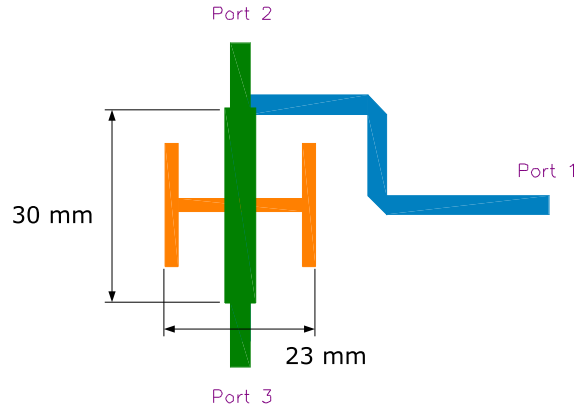


**Figure 16:** H-shaped aperture-coupled transition on 60-mil FR4 double layer substrate – Top view

### 2.3.2 Characterization and results

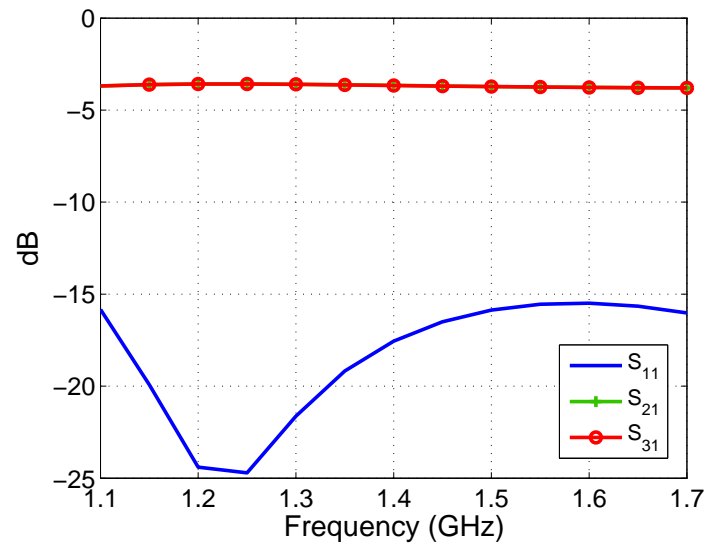
An H-shaped aperture-coupled transition has been fabricated to demonstrate the performance of the design. Two layers of 60-mil FR4 substrate have been used, and a  $10\ \mu\text{m}$  bonding film of FR4 equivalent material added to assemble the two layers (Fig. 18). The prototype is shown in Fig. 19. Characterized S-parameters and phase outputs are given in Fig. 20. The return loss is in agreement with simulation. Comparisons of simulated and measured output magnitudes and phase difference are given in Table 4. Output magnitude shows a maximum unbalance of 0.3 dB between 1.15 GHz and 1.6 GHz. A flat phase difference is observed in this frequency band.

	Amplitude $S_{21}/S_{31}$ (dB)		Phase diff. ( $^{\circ}$ )	
	Simu.	Charact.	Simu.	Charact.
1.15 GHz	-3.61/-3.61	-3.60/-3.93	180.0	180.4
1.35 GHz	-3.63/-3.63	-3.66/-3.93	180.0	180.5
1.6 GHz	-3.77/-3.77	-3.79/-3.93	180.0	180.3

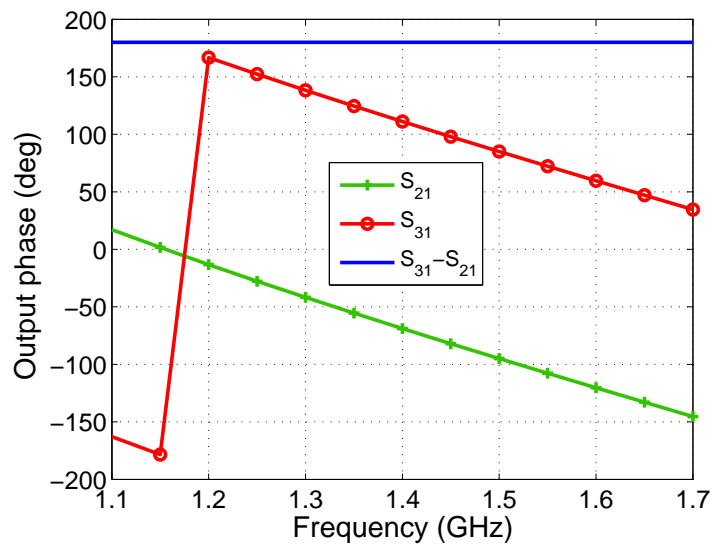
**Table 4:** Comparison of simulated and characterized results for the H-shaped aperture-coupled transition

## 2.4 Concluding remarks

Three microstrip  $180^{\circ}$  hybrids have been simulated around 1.37 GHz on FR4 substrate using different structures. The first one is the conventional ring hybrid. Its diameter is 59.58 mm and a 3-dB coupling with a maximum amplitude unbalance of less than 0.9 dB



(a)



(b)

**Figure 17:** H-shaped aperture-coupled transition  $S$ -parameters: (a) magnitude and (b) outputs phase.  $|S_{21}|$  and  $|S_{31}|$  curves are overlaid.



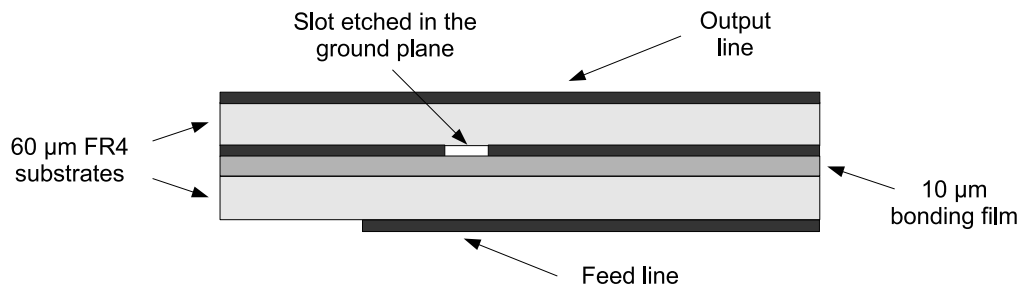


**Figure 18:** H-shaped aperture-coupled transition structure

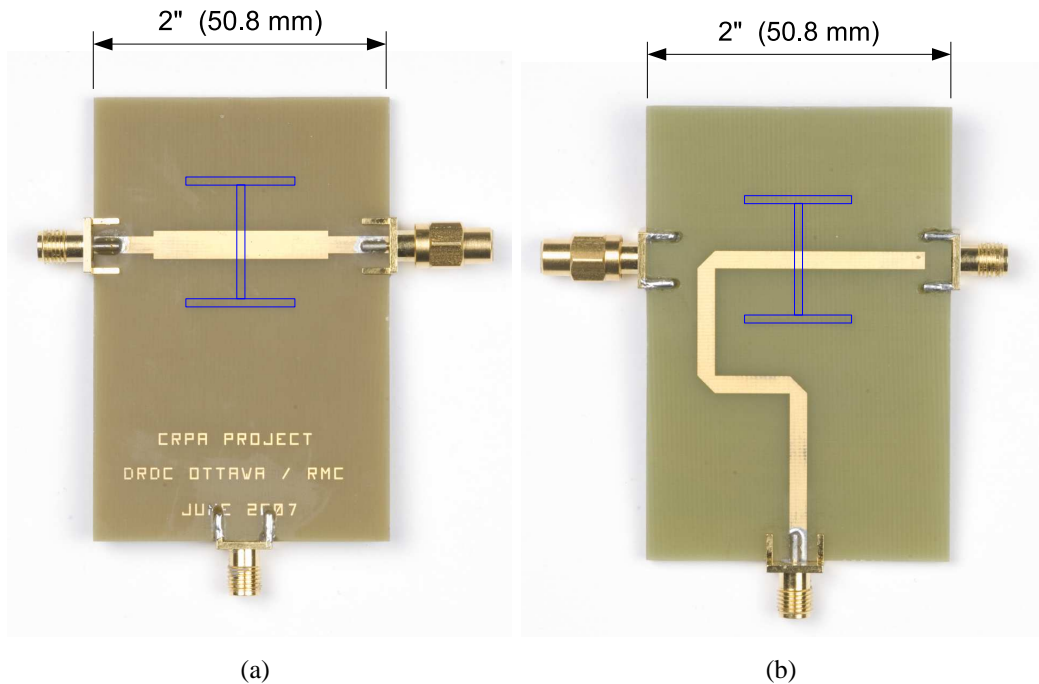
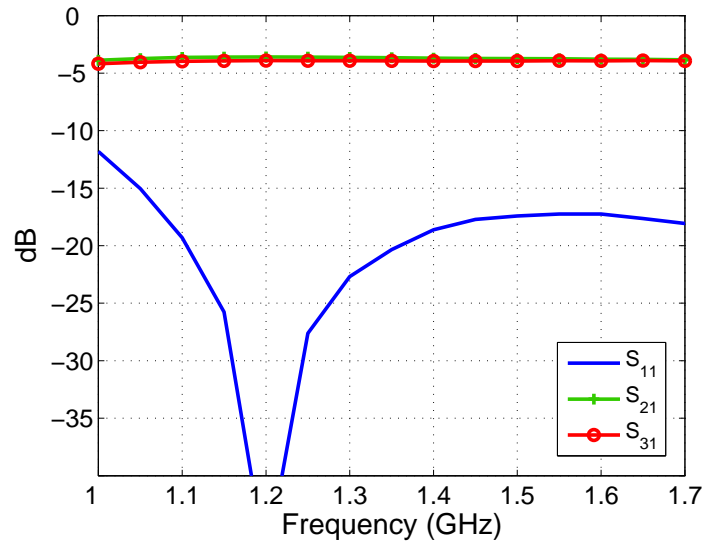


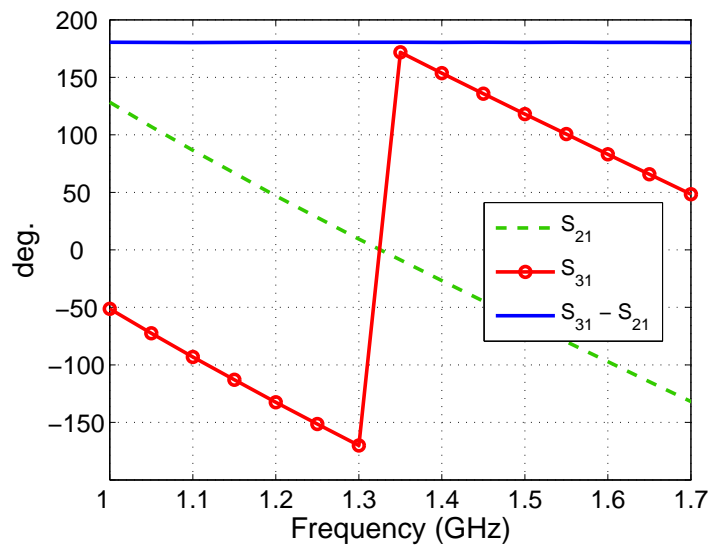
**Figure 19:** H-shaped aperture-coupled transition prototype (a) top and (b) bottom view – Thin lines show the position of the slot in the ground plane

between 1.15 and 1.6 GHz has been observed. Over this frequency band, the phase variation is  $23^\circ$ . To reduce the size, two fractal geometries of the ring hybrid have been investigated. The surfaces of these two couplers are 55 and 23 % respectively of the conventional ring hybrid's area and the performances on the 1.15-1.6 GHz frequency band are similar.

Additionally, an aperture-coupled transition has been used in a double layer structure. The shape of the slot is an 'H' to reduce the size and to improve the coupling. This geometry provides good performance on a broad frequency band. Between 1.15 and 1.6 GHz, the 3-dB maximum coupling amplitude unbalance is less than 0.3 dB and the phase variation is close to zero.



(a)



(b)

**Figure 20:** Characterization results of the H-shaped aperture-coupled transition  $S$ -parameters: (a) magnitude and (b) phase outputs

Figure 21 presents the different prototypes on the same scale allowing for direct size comparison. Good results have been obtained during characterization. Unbalanced amplitude 0.5 *dB* higher than simulation has been noted for the Moore 1-st iteration fractal hybrid. Small phase difference shifts have been observed for the hybrids.

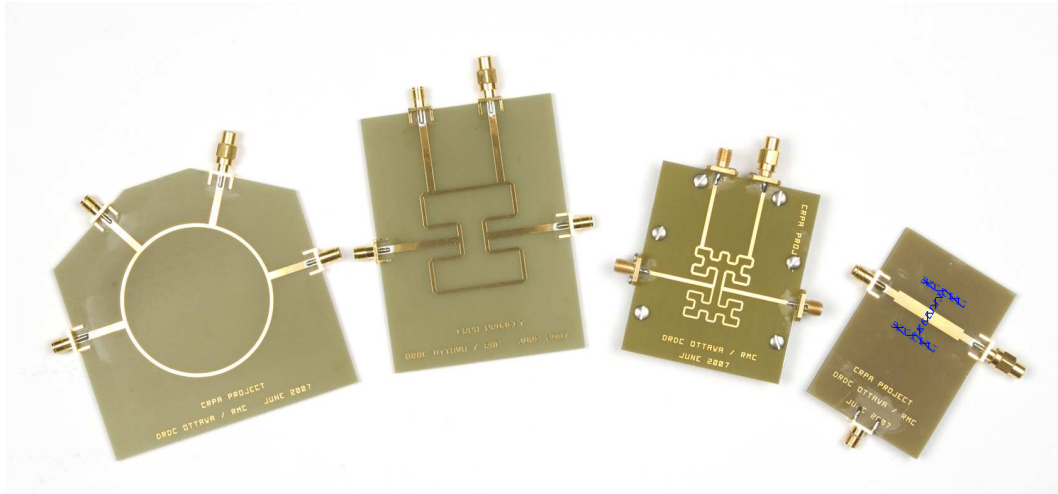


**Figure 21:** Hybrid designs on same scale using FR4 substrate

### 3 Simulation and characterization of 3-dB / 90° power splitters

---

Two types of miniaturization techniques have been investigated for the design of 3 dB / 90° microstrip splitters. Results presented here concern an investigation with a branch-line hybrid. The first method to reduce the size of the hybrid consists of using fractal geometries, as previously reported for the 3 dB / 180° hybrid. The second technique employs lumped distributed elements to decrease the size of a transmission line.

All simulations have been performed by taking material losses into account. No prototypes have been realized because this study is similar to the previous one with 180° power splitters, which has shown good agreement between simulation and characterization.

#### 3.1 Conventional 3-dB / 90° branch-line hybrid

The 90° printed branch-line hybrid includes four  $\lambda_g/4$  lines (with opposite sides parallel), with impedances of 50  $\Omega$  and 35.36  $\Omega$ , and 4 lines of 50  $\Omega$ . This forms a four-port network with a 90° phase shift between the two output ports.

Figure 22 shows the geometry and the convention for the ports. If the input is applied to port 1, the power will be evenly split into two components with a 90° phase difference at ports 3 and 4, and port 2 will be isolated. For more details on the functioning of this device, refer to [8].

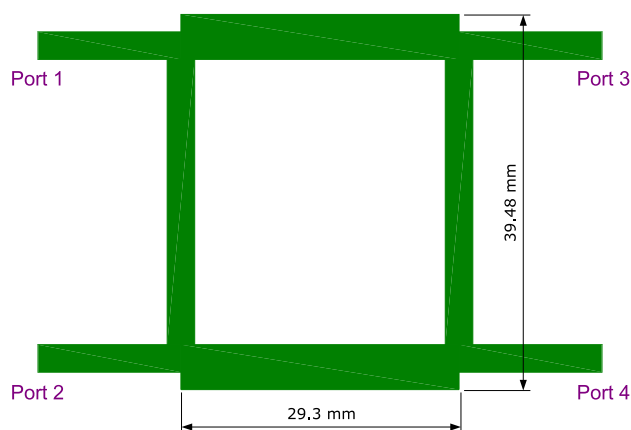
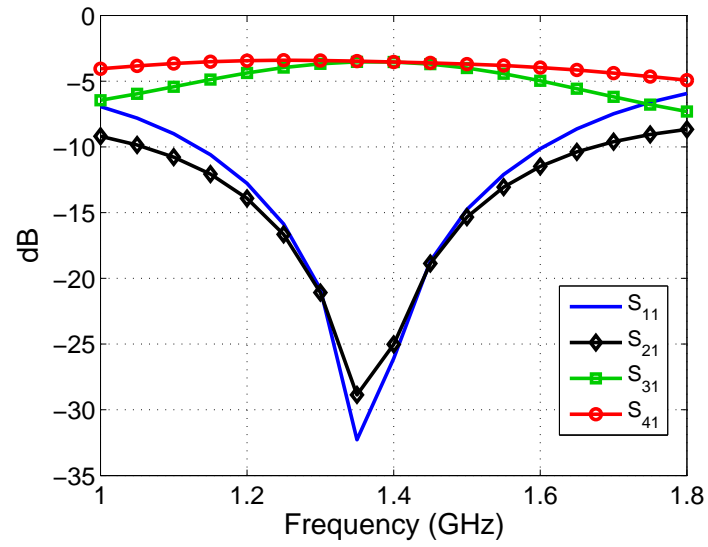


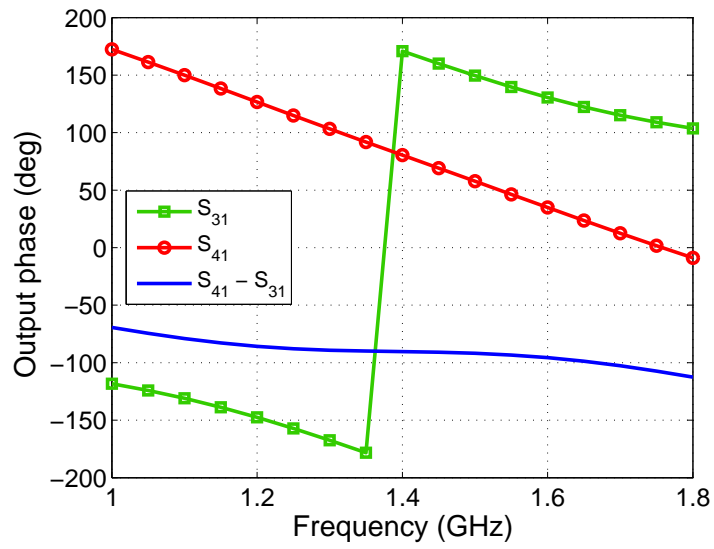
**Figure 22:** Microstrip branch-line hybrid on 60-mil FR4 substrate

Simulation results of S-parameters obtained for a 60-mil FR4 substrate ( $\epsilon_r = 4.4$ , and  $tg \delta = 0.009$ ) with the dimensions mentioned in Fig. 22 are presented in Fig. 23(a). Phase data are given in Fig. 23(b). One can notice that the frequency bandwidth is rela-

tively narrow, around 10 %. Considering this bandwidth, the coupling imbalance is 0.2 dB and the phase variation is  $2^\circ (\pm 1^\circ)$ .



(a)



(b)

**Figure 23:** Branch-line hybrid simulated  $S$ -parameters: (a) magnitude and (b) phase outputs

## 3.2 Fractal printed hybrid

Based on the results presented in section 2.2, fractal geometries have been considered here to miniaturize the branch-line hybrid. Sierpinski's shape has been chosen in this case.

### 3.2.1 Sierpinski 1-st iteration fractal hybrid

The first iteration of the Sierpinski's geometry has the shape of a 4-petal flower (Fig. 24). One can notice that this structure includes 16 segments. To find the length of a segment, the equation  $4 \text{ segments} = \lambda_g/4$  has to be solved. To take into account the width of the line, the length of the segment has to be shortened depending on the width of the line.

A branch-line hybrid has been implemented on a 60-mil FR4 substrate (Fig. 24). The impedances of the hybrid lines are  $50 \Omega$  and  $35.36 \Omega$ , which correspond to  $2.9 \text{ mm}$  and  $5.04 \text{ mm}$  respectively, for the selected substrate. The length of each segment has been adjusted to  $6.4 \text{ mm}$ . The four outputs have a  $50 \Omega$  line impedance.

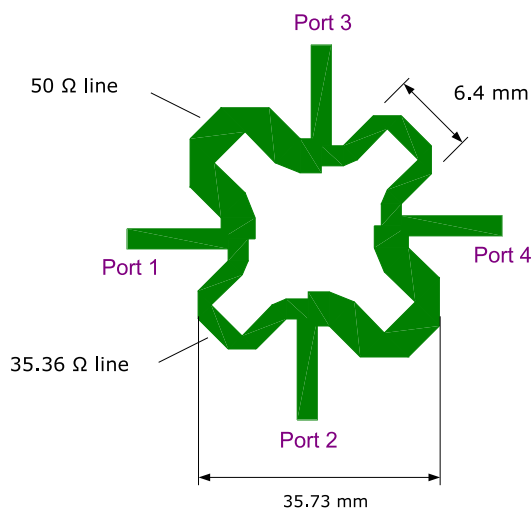
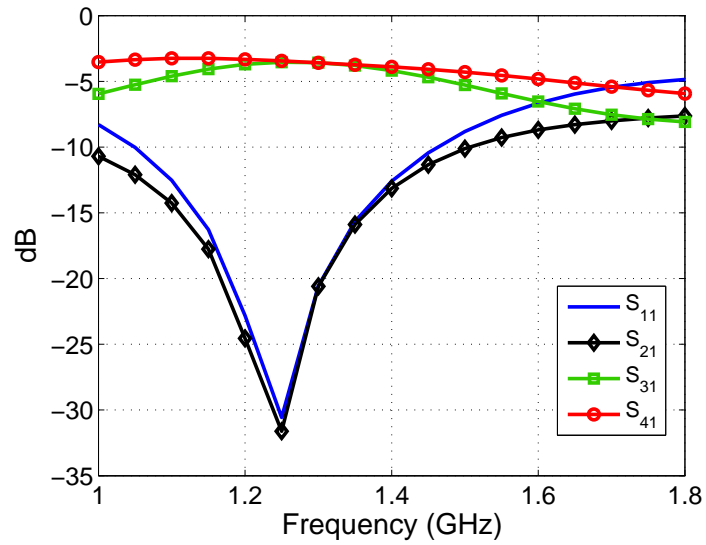


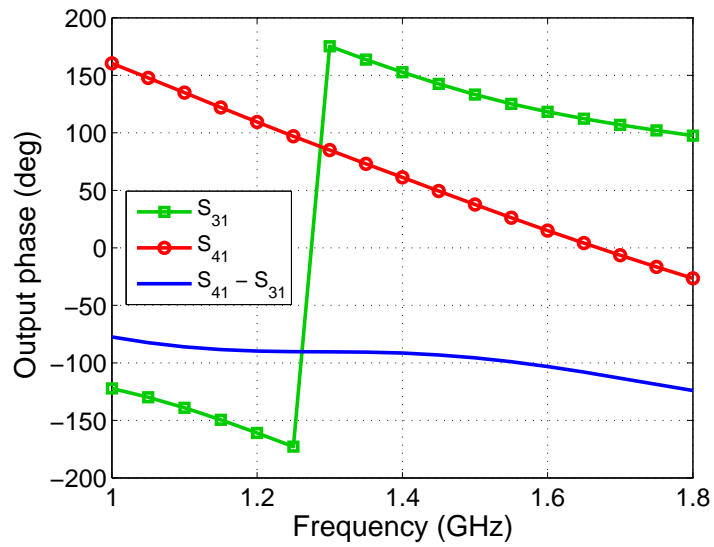
**Figure 24:** Sierpinski 1-st iteration  $90^\circ$  fractal hybrid on 60-mils FR4 substrate

Simulation results of S-parameters obtained for a 60-mil FR4 substrate with the dimensions mentioned in Fig. 24 are presented in Fig. 25(a). Phase data are given in Fig. 25(b). Here again, the frequency bandwidth is 10 % about, with a coupling imbalance of  $0.25 \text{ dB}$  and a phase variation of  $2^\circ (\pm 1^\circ)$ .

The sizes of the conventional branch-line hybrid and the 1st iteration Sierpinski fractal hybrid are similar.



(a)



(b)

**Figure 25:** Sierpinski 1-st iteration  $90^\circ$  fractal hybrid simulated  $S$ -parameters: (a) magnitude and (b) phase outputs

### 3.2.2 Sierpinski 2-nd iteration fractal hybrid

The second iteration of the Sierpinski's construction allows a reduction of the branch-line hybrid's area. Indeed, the perimeter of the central line is confined in a smaller frame because the construction includes more meanders (Fig. 26). This structure includes 64 segments corresponding to  $\lambda_g$ . In this case, the segment length is around  $1.6\text{ mm}$  at  $1.37\text{ GHz}$ . So far in this chapter, branch-line hybrids have been implemented on 60-mil FR4 substrate. The trace width corresponding to a  $35.36\ \Omega$  impedance equals  $5.04\text{ mm}$ . However, due to small segment lengths, the use of such a width is not practicable. To avoid such problems, the coupler could be designed with higher characteristic impedances ( $100$  and  $70.7\ \Omega$  for instance) and using quarter-wavelength lines for matching. But at  $1.37\text{ GHz}$ , the length of a quarter-wavelength line is significant (around  $30\text{ mm}$ ). Another solution is to implement the coupler on a 30-mil FR4 substrate. In this case, the width of the lines can be maintained and no additional matching is needed. The  $35.36\ \Omega$  segment of the fractal geometry segment on a 30-mil dielectric material is  $1.6\text{ mm}$  long and  $2.47\text{ mm}$  wide, the  $50\ \Omega$  segment is  $1.6\text{ mm}$  long and  $1.45\text{ mm}$  wide.

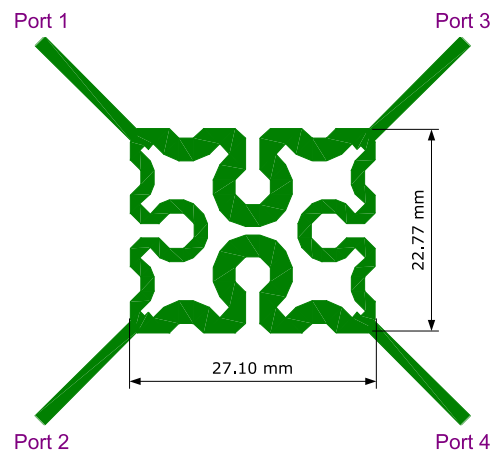


**Figure 26:** Sierpinski 2-nd iteration  $90^\circ$  fractal hybrid on 30-mil FR4 substrate

Compared to the conventional branch-line hybrid, similar simulation results have been obtained on a 30-mil FR4 substrate with the dimensions of Fig. 26. In the case of the Sierpinski 2-nd iteration, the obtained fractal geometry area is 53 % of the branch-line hybrid area. Figure 27 presents the different designs on the same scale allowing for direct size comparison.

One can note that the size reduction is achieved by decreasing the height. Another miniaturization technique will be presented in section 3.3 to reduce the width of the branch-line hybrid.



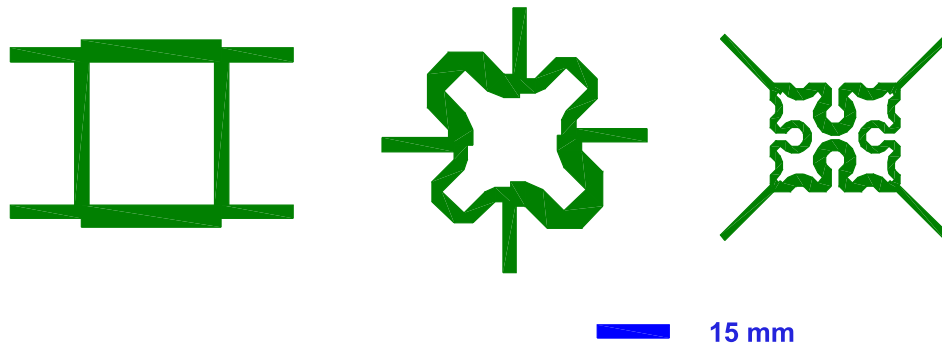


**Figure 27:** Hybrid designs on same scale using FR4 substrate

### 3.3 Lumped distributed elements

The use of lumped distributed elements is another miniaturization technique for reducing the size of a  $90^\circ$  branch-line hybrid [7]. This miniaturization method is presented in this section.

The lumped distributed elements method consists of shrinking a conventional transmission line having a  $Z_c$  impedance and a  $\theta$  electrical length (Fig. 28(a)) by replacing it by a shorter transmission line, of impedance  $Z_s$  and an electrical length of  $\theta_s$ , and two open stubs having a  $Z_{o1}$  impedance and a  $\theta_{o1}$  electrical length (Fig. 28(b)).

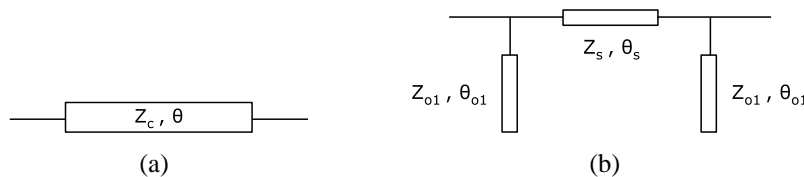


**Figure 28:** Size reduction scheme using lumped distributed elements. (a) Conventional transmission line. (b) Equivalent transmission line with a series transmission line and two open stubs.

Two design equations are needed to find the parameters of the equivalent transmission line:

$$B_{o1} = \frac{\cos \theta_s - \cos \theta}{Z_c \sin \theta} \quad (3.1)$$

$$Z_s = \frac{Z_c \sin \theta}{\sin \theta_s} \quad (3.2)$$

where  $B_{o1}$  is the input admittance of the open stubs defined by

$$j B_{o1} = j \tan \theta_{o1} / Z_{o1}. \quad (3.3)$$

The ratio  $\theta_s/\theta$  represents the size reduction factor. Knowing  $\theta$ ,  $\theta_s$  is fixed to have the desired reduction. The equivalent transmission line of Fig. 28(b) is a filter, so the cutoff frequency has to be considered. The authors of [7] show that  $\theta = 30^\circ$ ,  $\theta_s = 12.5^\circ$  associated with  $50 \Omega$  stubs allows wide-band applications as well as high cutoff frequency. Thus, the quarter-wavelength lines would be split into 3 segments.

### 3.4 Concluding remarks

Three microstrip  $90^\circ$  hybrids have been simulated around 1.37 GHz on FR4 substrate using different geometries. The first one is the conventional branch-line hybrid. Its size is  $29.3 \times 39.5 \text{ mm}^2$  and a 3-dB coupling with maximum amplitude unbalance of less than 0.2 dB between 1.32 and 1.47 GHz. Over this frequency band, the phase variation is  $2^\circ$  ( $\pm 1^\circ$ ).

To reduce the size, the lumped distributed elements method has been investigated. The size has been approximately divided by two with the second iteration of the Sierpinski fractal geometry. Compared to the conventional branch-line hybrid, similar simulation results have been obtained on a 30-mil FR4 substrate.

Finally, the lumped distributed elements miniaturization technique has been described. As for the fractal geometry technique, the size is divided by two, approximately, but here the length is reduced.

## 4 Conclusions and future work

---

Investigations into the miniaturization of 3-dB / 90 and 180° power splitters have been reviewed in this report. Several circuits and miniaturization techniques have been presented and used in the design of microstrip splitters.

Concerning the 3-dB / 180° splitters, two miniaturized microstrip circuits have been designed using two different methods. The first one is a Moore 2nd iteration fractal ring hybrid, of size  $23 \times 28 \text{ mm}^2$  (23 % of the conventional ring hybrid area) with similar performance over the 1.15-1.6 GHz frequency band. Over this band, characterization has shown a maximum 3-dB coupling imbalance of 1 dB and an output phase difference varying by 22° ( $\pm 11^\circ$ ). The second proposed circuit is an H-shaped aperture-coupled transition, of compact size and wide frequency bandwidth. Its size is  $23 \times 30 \text{ mm}^2$ , including the slot and matching network. Measurements revealed a maximum 3-dB imbalance of 0.3 dB and an output phase difference fluctuation of 1° ( $\pm 0.5^\circ$ ) over the 1.15-1.6 GHz band.

Characterization of the aperture-coupled transition involves some fabrication difficulties. For instance, the bonding film masks holes made for the probes, and pad associated with via holes are needed to access the ground for probe implantation. Technological solutions have been found but a longer design time is required during the circuit fabrication process.

Regarding the 90° splitters, two miniaturization methods have been investigated to reduce the size of a branch-line hybrid. The first technique is based on fractal geometries as for the 180° splitter. A Sierpinski 2nd iteration fractal branch-line hybrid has been simulated and showed a coupling imbalance of 0.4 dB and a phase difference variation of 1° ( $\pm 0.5^\circ$ ) over a 10 % bandwidth. Its size is about 50 % of the area of the branch-line hybrid. The second miniaturization technique that has been investigated is founded on lumped distributed elements to reduce the size of a microstrip line. The possible size reduction is 50 % as well.

Regarding future work, it is planned to do some tests with a substrate with dielectric losses lower than the FR4 substrate to see if the insertion loss could be improved. Moreover, other techniques can further reduce more the size of the circuits. For instance, coupled lines are integrable using Low Temperature Co-fired Ceramic (LTCC). Finally, the presented results concern narrowband circuits; for broad frequency band applications, the obtained performances are not sufficient, and the studied methods could be investigated as well to design wide-band circuits.

# References

---

- [1] K. Chang, editor (2005), Encyclopedia of RF and microwave engineering (pp. 1925-1935), John Wiley & Sons, Inc.
- [2] Hirota, T., Minakawa, A., and Muraguchi, M. (1990), Reduced-size branch-line and rat-race hybrids for uniplanar MMICs, *IEEE Trans. Microwave Theory Tech.*, 38(3), 270–275.
- [3] Ahn, H. R., Chang, I. S., and Yun, S. W. (1994), Miniaturized 3-dB ring hybrid terminated by arbitrary impedances, *IEEE Trans. Microwave Theory Tech.*, 42(12), 2216–2221.
- [4] Eccleston, K. W. and Ong, S. H. M. (2003), Compact planar microstripline branch-line and rat-race coupler, *IEEE Trans. Microwave Theory Tech.*, 51(10), 2119–2125.
- [5] Ghali, H. and Moselhy, T. A. (2004), Miniaturized Fractal Rat-Race, Branch-Line, and Coupled-Line Hybrids, *IEEE Trans. Microwave Theory Tech.*, 52(11), 2513–2520.
- [6] Ghali, H. and Moselhy, T. A. (2004), Design of Fractal Rat-Race Coupler, in *Proc. of International Microwave Symposium Digest MTT-S*, 1, 323–326.
- [7] Chun, Y.-H. and Hong, J.-S. (2006), Compact Wide-Band Branch-Line Hybrids, *IEEE Trans. Microwave Theory Tech.*, 54(2), 704–709.
- [8] Pozar, D. M. (2005), Microwave Engineering (3rd edition), John Wiley & Sons, Inc.
- [9] O. Lafond, O. Vendier Y. Cailloce, M. Himdi (2005), Thick-slot transition and antenna arrays in the Q band, *Microwave and Optical Technology Letters*, 44(1), 24–29.
- [10] Pozar, D. M. and Targonski, S. D. (1991), Improved coupling for aperture coupled microstrip antennas, *Electronics Letters*, 27(13), 1129–1131.

# Distribution list

---

DRDC Ottawa TM 2007-257

## Internal distribution

- 3 (2 HC + 1 CD) Michel Clénet (CNEW/Navigation)
- 4 (3 HC + 1 CD) Library
- 1 (CD) Jeff Bird (CNEW/Navigation)
- 1 (CD) Gilbert Morin (CNEW/Navigation)
- 1 (CD) Mike Vinnins (GL/CNEW/Navigation)
- 2 (HC + CD) Chen Wu (REW/Electronic Surveillance)

**Total internal copies: 12**

## External distribution

- 1 DRDKIM
- 3 (2 HC + 1 CD) Library and Archives Canada
- 1 (HC) Yahia M.M. Antar  
Royal Military College of Canada  
Dept. of Electrical and Computer Engineering  
P.O. Box 17000, Station Forces  
Kingston, ON, Canada  
K7K 7B4
- 1 (HC) Mathieu Caillet  
Royal Military College of Canada  
Dept. of Electrical and Computer Engineering  
P.O. Box 17000, Station Forces  
Kingston, ON, Canada  
K7K 7B4

**Total external copies: 6**

**Total copies: 18**

This page intentionally left blank.

**DOCUMENT CONTROL DATA**

(Security classification of title, body of abstract and indexing annotation must be entered when document is classified)

1. ORIGINATOR (The name and address of the organization preparing the document. Organizations for whom the document was prepared, e.g. Centre sponsoring a contractor's report, or tasking agency, are entered in section 8.) <b>Defence R&amp;D Canada – Ottawa 3701 Carling Avenue Ottawa, Ontario K1A 0Z4 Canada</b>		2. SECURITY CLASSIFICATION (Overall security classification of the document including special warning terms if applicable.) <b>UNCLASSIFIED</b>	
3. TITLE (The complete document title as indicated on the title page. Its classification should be indicated by the appropriate abbreviation (S, C or U) in parentheses after the title.) <b>Miniaturization of 3-dB / 90° and 180° power splitters using microstrip technology</b>			
4. AUTHORS (Last name, followed by initials – ranks, titles, etc. not to be used.) <b>Caillet, M.; Clénet, M.; Antar, Y.M.M.</b>			
5. DATE OF PUBLICATION (Month and year of publication of document.) <b>November 2007</b>		6a. NO. OF PAGES (Total containing information. Include Annexes, Appendices, etc.) <b>46</b>	6b. NO. OF REFS (Total cited in document.) <b>10</b>
7. DESCRIPTIVE NOTES (The category of the document, e.g. technical report, technical note or memorandum. If appropriate, enter the type of report, e.g. interim, progress, summary, annual or final. Give the inclusive dates when a specific reporting period is covered.) <b>Technical Memorandum</b>			
8. SPONSORING ACTIVITY (The name of the department project office or laboratory sponsoring the research and development – include address.) <b>Defence R&amp;D Canada – Ottawa 3701 Carling Avenue Ottawa, Ontario K1A 0Z4 Canada</b>			
9a. PROJECT NO. (The applicable research and development project number under which the document was written. Please specify whether project or grant.) <b>15bn01</b>		9b. GRANT OR CONTRACT NO. (If appropriate, the applicable number under which the document was written.)	
10a. ORIGINATOR'S DOCUMENT NUMBER (The official document number by which the document is identified by the originating activity. This number must be unique to this document.) <b>DRDC Ottawa TM 2007-257</b>		10b. OTHER DOCUMENT NO(s). (Any other numbers which may be assigned this document either by the originator or by the sponsor.)	
11. DOCUMENT AVAILABILITY (Any limitations on further dissemination of the document, other than those imposed by security classification.) <input checked="" type="checkbox"/> Unlimited distribution <input type="checkbox"/> Defence departments and defence contractors; further distribution only as approved <input type="checkbox"/> Defence departments and Canadian defence contractors; further distribution only as approved <input type="checkbox"/> Government departments and agencies; further distribution only as approved <input type="checkbox"/> Defence departments; further distribution only as approved <input type="checkbox"/> Other (please specify):			
12. DOCUMENT ANNOUNCEMENT (Any limitation to the bibliographic announcement of this document. This will normally correspond to the Document Availability (11). However, where further distribution (beyond the audience specified in (11)) is possible, a wider announcement audience may be selected.)			

13. ABSTRACT (A brief and factual summary of the document. It may also appear elsewhere in the body of the document itself. It is highly desirable that the abstract of classified documents be unclassified. Each paragraph of the abstract shall begin with an indication of the security classification of the information in the paragraph (unless the document itself is unclassified) represented as (S), (C), (R), or (U). It is not necessary to include here abstracts in both official languages unless the text is bilingual.)

This document reports on the analysis and design of miniaturized 3-dB / 90° and 180° power splitters. Several miniaturization techniques are presented, and were applied to the design of microstrip splitters.

Concerning the 3-dB / 180° splitters, two miniaturized microstrip circuits have been designed using two different methods. The first one is a Moore 2nd iteration fractal ring hybrid, of size  $23 \times 28 \text{ mm}^2$  (23 % of the conventional ring hybrid area) with similar performance over the 1.15-1.6 GHz frequency band. Over this band, characterization has shown a maximum 3-dB coupling imbalance of 1 dB and an output phase difference varying by  $22^\circ (\pm 11^\circ)$ . The second proposed circuit is an H-shaped aperture-coupled transition, of compact size and wide frequency bandwidth. Its size is  $23 \times 30 \text{ mm}^2$ , including the slot and matching network. Measurements revealed a maximum 3-dB imbalance of 0.3 dB and an output phase difference fluctuation of  $1^\circ (\pm 0.5^\circ)$  over the 1.15-1.6 GHz band.

Regarding the 90° splitters, two miniaturization methods have been investigated to reduce the size of a branch-line hybrid. The first technique is based on fractal geometries as for the 180° splitter. A Sierpinski 2-nd iteration fractal branch-line hybrid has been simulated and showed a coupling imbalance of 0.4 dB and a phase difference variation of  $1^\circ (\pm 0.5^\circ)$  over a 10 % bandwidth. Its size is about 50 % of the area of the branch-line hybrid. The second miniaturization technique that has been investigated is founded on lumped distributed elements to reduce the size of a microstrip line. The possible size reduction is 50 % as well.

14. KEYWORDS, DESCRIPTORS or IDENTIFIERS (Technically meaningful terms or short phrases that characterize a document and could be helpful in cataloguing the document. They should be selected so that no security classification is required. Identifiers, such as equipment model designation, trade name, military project code name, geographic location may also be included. If possible keywords should be selected from a published thesaurus. e.g. Thesaurus of Engineering and Scientific Terms (TEST) and that thesaurus identified. If it is not possible to select indexing terms which are Unclassified, the classification of each should be indicated as with the title.)

180° power splitter  
90° power splitter  
hybrids  
miniaturization  
microstrip technology  
aperture-coupled transition





## **Defence R&D Canada**

Canada's leader in Defence  
and National Security  
Science and Technology

## **R & D pour la défense Canada**

Chef de file au Canada en matière  
de science et de technologie pour  
la défense et la sécurité nationale



[www.drdc-rddc.gc.ca](http://www.drdc-rddc.gc.ca)